

## Effect of reactant spatial distribution in the $A + B \rightarrow 0$ reaction kinetics in one dimension with Coulomb interaction

V. N. Kuzovkov,<sup>1,2</sup> E. A. Kotomin,<sup>1,3</sup> and W. von Niessen<sup>2</sup>

<sup>1</sup>University of Latvia, Rainis Boulevard 19, Riga LV-1586, Latvia

<sup>2</sup>Institut für Physikalische und Theoretische Chemie, Technische Universität Braunschweig, D-38106 Braunschweig, Germany

<sup>3</sup>Institute of Physics and Astronomy, Aarhus University, Aarhus-C, DK-8000, Denmark

(Received 9 July 1996)

The effect of nonequilibrium charge screening in the kinetics of the one-dimensional, diffusion-controlled  $A + B \rightarrow 0$  reaction between charged reactants in solids and liquids is studied. The incorrectness of the static, Debye-Hückel theory is shown. Our microscopic formalism is based on the Kirkwood superposition approximation for three-particle densities and the self-consistent treatment of the electrostatic interactions defined by the nonuniform spatial distribution of similar and dissimilar reactants treated in terms of the relevant joint correlation functions. Special attention is paid to the pattern formation due to a reaction-induced non-Poissonian fluctuation spectrum of reactant densities. This reflects a formation of loose domains containing similar reactants only. The effect of asymmetry in reactant mobilities ( $D_A = 0$ ,  $D_B > 0$ ) contrasting the traditional symmetric case, i.e., equal diffusion coefficients ( $D_A = D_B$ ), is studied. In the asymmetric case concentration decay is predicted to be *accelerated*,  $n(t) \propto t^{-\alpha}$ ,  $\alpha = \frac{1}{3}$ , as compared to the well-established critical exponent for fluctuation-controlled kinetics in the symmetric case,  $\alpha = \frac{1}{4}$ , and/or the prediction of the standard chemical kinetics,  $\alpha = \frac{1}{2}$ . Results for the concentration decay and growth under permanent particle source are compared with results of the mesoscopic theory. [S1063-651X(96)08112-3]

PACS number(s): 05.40.+j, 05.70.Ln, 64.60.Cn, 82.20.Mj

### I. INTRODUCTION

Bimolecular  $A + B \rightarrow 0$  reactions are quite common in condensed matter physics and physical chemistry; e.g., they occur between primary radiation defects of two types,  $A$  and  $B$ , which recombine when they approach each other during diffusion walks to within some critical distance  $r_0$ . These particles (Frenkel defects in solids and/or electrons and radicals in liquids) could be neutral or charged. Empty anion vacancies  $V_a$  and complementary interstitial anions  $X^-$  (the so-called  $I$  centers), as well as  $F$  centers ( $V_a$  which trapped an electron) and  $X^0$  interstitial atoms (called  $H$  centers) could serve as examples of charged or neutral defects in irradiated alkali-metal halide crystals,  $\text{MeX}$ .

Many-particle effects caused by the spatial fluctuations of the reactant densities have been intensively studied in recent years in the kinetics of bimolecular chemical reactions, including the above-mentioned  $A + B \rightarrow 0$  reaction. A number of quite different techniques and methods were developed for this purpose, including direct computer simulations [1], a mesoscopic approach [2,3], and scaling [4], as well as microscopic theory [5–7] (see also references in [8] and review articles [6,7]). These studies clearly demonstrated that the kinetic laws established long ago in standard chemical kinetics [9] could be violated, usually at high particle concentrations or long reaction times. In particular, the asymptotic ( $t \rightarrow \infty$ ) concentration decay rate turns out to be  $n(t) \propto t^{-d/4}$ , where  $d \leq 4$  is the spatial dimension; i.e., it is *slower* than the one in standard chemical kinetics,  $\alpha = \frac{1}{2}$  and 1 and 1 for  $d = 1, 2$ , and 3, respectively. This effect, called sometimes abnormal kinetics—abnormal from the standard point of view—is directly related to the reaction-induced nonuniform reactant distribution which is in contrast to the

main prediction of chemical kinetics that all reactants are well stirred, and the reaction volume is homogeneous. As a result, modern chemical kinetics uses the language of *critical exponents*, *correlation lengths*, etc., similar to the physics of critical phenomena.

Presently almost all studies of fluctuation-controlled effects deal with neutral, noninteracting particles, thus neglecting effects caused by their interaction. Rare exceptions are to be found in Refs. [5,10–15]. In this paper, we study many-particle effects between charged reactants, and show that the generalization of the formalism developed earlier for neutral particles, to the case of charged particles is not always trivial, and requires a careful restatement of the problem.

Two basic approaches to the fluctuation-controlled kinetics are widely used nowadays: they are known as mesoscopic [10–12] and microscopic [5,6,13–15] approaches. The former does not treat the reaction event at all and focuses on the calculation of the reaction *asymptotics* at long reaction times,  $t \rightarrow \infty$ . As stated above, the critical exponent  $\alpha$  in the algebraic decay law for the reactant concentration depends on the space dimension  $d$  only. It is defined entirely by the large-scale reactant density fluctuations characterized by the length parameter called the *diffusion length*,  $\xi(t) = \sqrt{Dt}$ , where  $D = D_A + D_B$  is the coefficient of the relative diffusion. At long reaction times,  $\xi(t)$  exceeds any final length parameter in the reaction system (e.g., the reaction radius  $r_0$  or radius of the effective reaction,  $R_{\text{eff}}$ , between interacting particles) and governs the kinetics.

The mesoscopic studies [10–12] are a good illustration of what was stated above. The authors, following a pioneering approach [2], reduced the kinetic problem to a study of a single nonlinear stochastic equation of the following kind:

$$\frac{\partial q}{\partial t} = (D + w|q|)\Delta q + w\text{sgn}(q)(\nabla q)^2 + i, \quad (1)$$

where  $q(\mathbf{r}, t) = C_A(\mathbf{r}, t) - C_B(\mathbf{r}, t)$  is a local difference in reactant densities (particle concentrations),  $w$  a parameter characterizing particle interaction ( $w \sim D/k_B T$ ), and  $i$  a stochastic particle flux in the  $d$ -dimensional volume (in the case of particle production). When deriving Eq. (1), the macroscopic concentrations were assumed to be equal,  $n_A = n_B = n(t)$ , these concentrations are average values of the local concentrations,  $n_\nu = C_\nu(r, t)$  and  $\nu = A$  and  $B$ . Proceeding in this way, the time development of the macroscopic concentration  $n(t)$  could be expressed through the mean value of the stochastic variable  $q(\mathbf{r}, t)$  and thus the critical exponents could be calculated for both cases—the concentration decay after pulsed particle creation ( $i=0$ ), and the kinetics under the permanent particle source.

In order to solve the kinetic problem analytically, additional symmetry assumptions are imposed on the diffusion coefficients  $D_A = D_B$  and the interaction potentials  $U_{\lambda\mu}(r) = \pm e_\lambda e_\mu u(r/r_m)$ , where  $u(x)$  is some function and  $|e_\nu| = e$ . Moreover,  $u(x)$  is assumed to be integrable, and characterized by a finite action radius  $r_m$ . The two symmetry conditions allow us to reduce the number of nonlinear stochastic equations to be solved to one, whereas due to the potential integrability condition the equation derived has no nonlocal terms and permits us to characterize particle interaction by a single parameter  $w$ .

However, these mathematical assumptions are often in conflict with the actual *physical* problem. In particular, the mobility of the above-mentioned interstitial atoms typically exceeds that of vacancies by 10–15 orders of magnitude [16]. Moreover, in the case of the elastic interaction typical for neutral particles, caused by the overlap of the lattice deformation fields around two close defects,  $|U_{AA}(r)| \neq |U_{BB}(r)| \neq |U_{AB}(r)|$ . The interaction is attractive for pairs of *both* similar ( $AA, BB$ ) and dissimilar ( $AB$ ) particles. This means that the parameter  $w$  in Eq. (1) is negative. As noted in [10], in this case a singular solution occurs due to a collapse in the system of similar particles. This demonstrates clearly that the mesoscopic approach fails in the cases where *small-scale* density fluctuations are important, and thus one can no longer avoid the detailed treatment of the particle interactions.

The above-mentioned collapse indeed manifests itself experimentally in the form of aggregates (colloids) of similar radiation defects [17,18]. It is clear that the critical exponent itself is not well suited for describing aggregation processes: under permanent irradiation defect concentrations saturate at some time,  $n(t \rightarrow \infty) = n_s = \text{const}$ . This means that the result of the relevant discrete-lattice treatment of defects (taking into account their finite sizes) is trivial,  $\alpha \rightarrow 0$ . On the other hand, it is known experimentally that the aggregation process consists of many subsequent stages—the formation of defect pairs (dimers), trimers, etc. is observed as time increases. That is, *spatiostructural* properties, such as the time development of a single defect concentration, that of dimers, etc., the mean size of aggregates and the number of particles inside it become of great importance. Moreover, these properties are closely related to the time development of the char-

acteristic correlation functions defining the relative spatial distribution of particles and the relevant *pattern formation* kinetics. We demonstrate below that the same is true for the Coulomb interaction—a better understanding of peculiarities in the kinetics due to many-particle effects can be achieved through the detailed treatment of the time development of the spatial reactant distribution.

The particle aggregation problem does not arise in the mesoscopic theory for  $w > 0$  (similar particle repulsion). Good example of such a situation is a screened Coulomb interaction (the Debye-Hückel potential) which guarantees potential symmetry and integrability [10]. In this paper, we study in detail the effects of *dynamical* Coulomb potential screening in the  $A + B \rightarrow 0$  reaction. In the following we show that the additional assumption of the mesoscopic theory about potential integrability in fact is *not* fulfilled. Depending on the particular mobility case (symmetric and/or asymmetric) the asymptotic behavior of the reactant concentrations can be either similar to a system of noninteracting particles, or quite different (which is a direct consequence of the infinite-radius potential).

Since the case of  $d=3$  has been analyzed by us in Ref. [14], in the present paper we study the reaction peculiarities for *low* dimensions, focusing on  $d=1$  (reaction in capillaries). It will be shown that in this case the reaction radius  $r_0$  could be set to zero, which allows us to eliminate this parameter and to compare directly our results with the mesoscopic theory [10–12]. We also study the particle *accumulation* kinetics where the mesoscopic theory predicts deviations from reaction kinetics known for neutral particles.

The paper is organized as follows. In Sec. II a set of nonlinear kinetic equations for arbitrary space dimension  $d$  is presented, and its simplification for low dimensions is discussed. The screened interaction potentials are derived in Sec. III, in the spirit of the Debye-Hückel approach in statistical physics of dense Coulomb systems. The key point here is that our effective potentials are *dynamical*, and directly related to the time development of the spatial reactant distribution. The reaction equations obtained are rewritten in dimensionless form in Sec. IV. Particle accumulation kinetics is studied in Sec. V. Section VI presents an analysis of the main results obtained, and their comparison with the mesoscopic theory. The Appendix summarizes important details of our difference scheme used for the nontrivial numerical solution of nonlinear kinetic equations with singular potentials.

## II. KINETIC EQUATIONS

The basic equations of our microscopic theory of interacting particles have been derived and discussed recently for  $d=3$  for the cases of Coulomb [14] and elastic [ $U(r) \propto 1/r^3$ ] [15] interactions. Now, based on results of a review article [7], we generalize these equations for an arbitrary space dimension  $d$ . This helps us to show peculiarities in the transition to low dimensions.

Use of the Kirkwood superposition approximation [19] for decoupling the infinite hierarchy of equations for the correlation functions leads to a minimum set of variables describing the fluctuation-controlled reaction kinetics. These are the macroscopic concentrations  $n_A = n_B = n(t)$ , and three kinds of *joint correlation functions* [6,7]—two for similar particles,

$X_\nu(r,t)$  and  $\nu=A$  and  $B$ , and a third one for dissimilar particles,  $Y(r,t)$ , where  $r$  is the relative distance between two particles. These functions describe a spatial distribution of pairs  $AA$ ,  $BB$ , and  $AB$ , respectively, and are analogous to the radial distribution function in statistical physics of dense gases and liquids [20]. The physical meaning of these correlation functions is the following [7,14]:  $C_A^{(a)}(r,t) = n(t)X_A(r,t)$  and  $C_B^{(a)}(r,t) = n(t)Y(r,t)$  are mean densities of particles  $A$  and  $B$ , respectively, at the relative distance  $r$ , provided that a probe particle  $A$  is in the coordinate origin. Introducing for simplicity a function  $X(r,t) = (X_A(r,t) + X_B(r,t))/2$  the basic set of kinetic equations reads:

$$\frac{dn(t)}{dt} = -K(t)n^2(t), \quad K(t) = \gamma_d r_0^{d-1} |\mathbf{j}(r_0, t)|, \quad (2)$$

$$\partial Y(r,t)/\partial t = \nabla \cdot \mathbf{j}(r,t) - 2n(t)K(t)Y(r,t)J_d[X], \quad (3)$$

$$\mathbf{j}(r,t) = (D_A + D_B) \{ \nabla Y(r,t) + \beta \nabla U'_{AB}(r,t) Y(r,t) \}, \quad (4)$$

$$\partial X_\nu(r,t)/\partial t = \nabla \cdot \mathbf{j}_\nu(r,t) - 2n(t)K(t)X_\nu(r,t)J_d[Y], \quad (5)$$

$$\mathbf{j}_\nu(r,t) = 2D_\nu \{ \nabla X_\nu(r,t) + \beta \nabla U'_{\nu\nu}(r,t) X_\nu(r,t) \}. \quad (6)$$

In Eqs. (2)–(6) the black-sphere recombination model is assumed implicitly: any  $AB$  pair recombines instantly when two reactants during their diffusive walks approach each other to within some critical distance  $r_0$  [6,7]. This fact is incorporated into the (Smoluchowski) boundary condition for the correlation function of dissimilar particles;  $Y(r \leq r_0, t) = 0$  in Eq. (3). This correlation function defines the quantity of primary importance—the *reaction rate*  $K(t)$  which is a flux of particles over the recombination sphere's surface ( $\gamma_d = 2, 2\pi$ , and  $4\pi$  for  $d = 1, 2, 3$ , respectively). For a finite  $r_0$  the reaction rate reads

$$K(t) = \gamma_d r_0^{d-1} \partial Y(r,t)/\partial r|_{r=r_0}.$$

The nonlinear terms in Eqs. (3) and (5) containing the functionals  $J_d[Z]$  arise directly from the Kirkwood approximation [19] (see [6,7,14]). Their expressions for  $d = 1, 2$ , and 3 are given in Ref. [7]. In particular,

$$J_1[Z] = (Z(r+r_0, t) + Z(|r-r_0|, t))/2 - 1. \quad (7)$$

Expressions for the flux densities  $\mathbf{j}(r,t)$  and  $\mathbf{j}_\nu(r,t)$  ( $\beta = 1/k_B T$ ) are also nonlinear, since the effective potential energies  $U'_{\lambda\mu}(r,t)$  receive contributions of both direct ( $\lambda\mu$  pair) and indirect lateral particle interactions through surrounding particles. The technique for their calculation in the case of a short-range potential has been discussed in Ref. [15], and that for the Coulomb potentials in Ref. [14].

Low-dimensional ( $d = 1$  and  $2$ ) systems with Coulomb interaction reveal a peculiarity which allows us to reduce the number of independent variables and to simplify the kinetic equations. That is, we can perform the limiting transition  $r_0 \rightarrow 0$ , retaining the finite reaction rate. Physically this means that the reaction rate is governed by the effective radius. This radius is the largest one of the scale lengths in the system. For the Coulomb systems such a scale is called the *Onsager radius*,  $R = e^2/\epsilon k_B T$  [14]. This is a distance at

which the thermal energy equals the attraction energy; when approaching to within  $R$  two reactants cannot separate, and thus they inevitably recombine. Usually  $R \gg r_0$  and thus  $R$  determines the reaction rate. Neglecting many-particle effects, the latter has a very simple form:  $K = 4\pi DR_{\text{eff}}$  [7,9]. In the limiting case of  $r_0 \rightarrow 0$  the functional  $J_d[Z]$  in Eqs. (3) and (5) is greatly simplified,

$$J_d[Z] = Z(r,t) - 1.$$

This limiting transition is also very useful for the study of accumulation kinetics (Sec. V).

### III. EFFECTIVE COULOMB INTERACTION: DYNAMICAL CHARGE SCREENING

Consider now the calculation of the particle electrostatic interactions in low dimensions taking place on a surface ( $d = 2$ , motion on the  $xy$  plane) or in capillaries ( $d = 1$ , motion along the  $x$  axis). Rewrite the Poisson equation

$$\Delta \phi(x,y,z) = -\frac{4\pi}{\epsilon} \rho(x,y,z) \quad (8)$$

in the integral form

$$\phi(\mathbf{r}) = \int \frac{\rho(\mathbf{r}')}{\epsilon |\mathbf{r} - \mathbf{r}'|} dx dy dz. \quad (9)$$

Following the well-known Debye-Hückel approach [20] let us place a probe charge  $e_\nu$  in the coordinate origin, which induces the excess charge density  $\rho_\nu(\mathbf{r}, t)$ , and calculate the relevant effective potential  $\phi_\nu(\mathbf{r}, t)$ . In  $d = 3$ , due to a spherical symmetry of the induced charge distribution this problem has a simple solution [20]. The differential form of the Poisson equation is very convenient for the numerical calculations [14]. In  $d = 2$  one is interested in the potential on the surface,  $\Phi_\nu(r, t)$  with  $r = \sqrt{x^2 + y^2}$ . The obvious ansatz here is a substitution for the induced charge density  $\rho_\nu(x,y,z,t) = \sigma_\nu(r,t) \delta(z)$ , where  $\sigma_\nu(r,t)$  is a two-dimensional charge density at the distance  $r$  from the coordinate origin, and  $\delta$  is the Dirac delta function.

More delicate is the situation in  $d = 1$ , where one needs to find the potential along the  $x$  axis,  $\Phi_\nu(r, t)$  where  $r = |x|$ . The trivial treatment of the  $1d$  string with  $\rho_\nu(x,y,z,t) = \sigma_\nu(r,t) \delta(y) \delta(z)$ , where  $\sigma_\nu(r,t)$  is the  $1d$  charge density, fails, since the potential of a charged string is singular (logarithmically divergent) on this string. That is, the case  $d = 1$  should be considered as a quasi- $1d$  motion where the particle coordinates have some distribution along the  $y$  and  $z$  axes (a capillary of the finite radius  $r_c$ ) but the recombination is governed by the  $x$  coordinate. In a one-parameter model, one obtains

$$\Phi_\nu(r,t) = \frac{e_\nu}{\epsilon r} + \int \frac{\sigma_\nu(|z'|, t)}{\epsilon \sqrt{(r-z')^2 + r_c^2}} dz'. \quad (10)$$

Equation (10) contains the potential of a probe charge  $e_\nu$  placed in the coordinate origin, and assumes that the induced charge is distributed symmetrically with respect to the coordinate origin. In other words, Eq. (10) describes the case

where the screening particles are distributed over the capillary surface with a radius  $r_c$ . For the self-consistent calculation of the induced potential, Eq. (10) should be extended by the effective density of induced charges. For this purpose the physical meaning of the correlation function should be used (Sec. II): the mean charge densities of  $A$  and  $B$  particles are nothing but

$$e_A C_A^{(a)}(r, t) = e_A n(t) X_A(r, t)$$

and

$$e_B C_B^{(a)}(r, t) = e_B n(t) Y(r, t),$$

respectively, provided that a probe particle  $A$  is in the coordinate origin. Since  $e = e_A = -e_B$ , one obtains a charge density induced by a particle of type  $\nu$

$$\sigma_\nu(r, t) = e_\nu n(t) (X_\nu(r, t) - Y(r, t)). \quad (11)$$

The effective potential interaction energies in Eqs. (4) and (6) are

$$U'_{\nu\nu}(r, t) = e_\nu \Phi_\nu(r, t)$$

and

$$U'_{AB}(r, t) = -(U'_{AA}(r, t) + U'_{BB}(r, t))/2,$$

respectively. That is, the spatial distribution of  $A$  and  $B$  particles described in terms of the joint correlation functions determines the spatial charge distribution and the relevant potentials (10) in which these charges are moving. In other words, we have a *self-consistent* treatment of particle motion and the potentials where they move.

#### IV. DIMENSIONLESS KINETIC EQUATIONS

After eliminating the reaction radius  $r_0$  two (one) length scale remains in the kinetic problem: in the  $1d$  case the capillary radius  $r_c$  and the Onsager radius  $R$ , or, in the  $2d$  case, only the Onsager radius  $R$ . It is convenient to introduce the dimensionless parameters  $r' = r/R$ ,  $r'_c = r_c/R$ ,  $t' = Dt/R^2$ ,  $D'_\nu = 2D_\nu/D$ ,  $n'(t') = \gamma_d r_0^d n(t)$ ,  $U_\nu(r', t') = \beta U'_{\nu\nu}(r, t)$ , and  $U(r', t') = \beta U'_{AB}(r, t)$ .

In variables (primes are omitted below) our kinetic equations read

$$\frac{dn(t)}{dt} = -K(t)n^2(t), \quad K(t) = \lim_{r \rightarrow 0} j(r, t), \quad (12)$$

$$\partial Y(r, t) / \partial t = \partial j(r, t) / \partial r - 2n(t)K(t)Y(r, t)[X(r, t) - 1], \quad (13)$$

with

$$j(r, t) = \partial Y(r, t) / \partial r + \partial U(r, t) / \partial r Y(r, t), \quad (14)$$

and

$$\partial X_\nu(r, t) / \partial t = \partial j_\nu(r, t) / \partial r - 2n(t)K(t)X_\nu(r, t)[Y(r, t) - 1], \quad (15)$$

with

$$j_\nu(r, t) = D_\nu \{ \partial X_\nu(r, t) / \partial r + \partial U_\nu(r, t) / \partial r X_\nu(r, t) \}. \quad (16)$$

The Smoluchowski boundary condition for Eq. (13) is

$$Y(0, t) = 0. \quad (17)$$

The boundary condition for similar particles,

$$\lim_{r \rightarrow 0} j_\nu(r, t) = 0, \quad (18)$$

means that  $AA$  and  $BB$  particle pairs do not interact, but reflect each other upon particle collisions (we neglect the size of the particles).

Due to the short-range nature of the spatial particle correlations and the normalization condition, one obtains

$$\lim_{r \rightarrow \infty} Y(r, t), X_\nu(r, t) = 1. \quad (19)$$

We assume a random initial distribution of reactants,

$$X_\nu(r, 0) = Y(r, 0) = 1.$$

The set of Eqs. (12), (13), and (15) has to be extended by the effective interaction potentials. In  $1d$  these potentials are

$$U_\nu(r, t) = 1/r + n(t) \int_0^\infty G(r, r'; r_c) [X_\nu(r', t) - Y(r', t)] dr', \quad (20)$$

where

$$G(r, r'; r_c) = \{ [(r - r')^2 + r_c^2]^{-1/2} + [(r + r')^2 + r_c^2]^{-1/2} \} / 2. \quad (21)$$

Therefore, the recombination kinetics is defined by the following dimensionless parameters: (i) the initial particle concentration  $n(t=0) = n(0)$ , (ii) the *partial* diffusion coefficient  $\kappa = D_A/D$  [note that dimensionless diffusion coefficients are related by the condition  $D_A + D_B = 2$ , i.e.  $D_A = 2\kappa$ ,  $D_B = 2(1 - \kappa)$ ], and (iii) the capillary radius  $r_c$  (in the  $1d$  case).

As is well known, the asymptotic decay law does not depend on the initial particle concentration. The latter defines only the critical time when such an asymptotics occurs: the larger  $n(0)$ , the shorter a transient time. In contrast, the asymptotic law could depend on the relative mobility parameter  $\kappa$  since a difference in particle diffusion coefficients leads to different spatial distributions,  $X_A(r, t) \neq X_B(r, t)$ . The same is true for the particle screening, Eq. (21).

#### V. PARTICLE PRODUCTION

Let us now incorporate into the kinetic equations the effect of permanent particle production with the rate  $p$  per volume unit and time. An example is a production of Frenkel defects in solids under irradiation [16]. We neglect the initial spatial correlation within *geminat*  $AB$  pairs of dissimilar particles created simultaneously (high energy irradiation). As is known [21], the main problem of the accumulation kinetics arises in the calculation of the volume fraction occupied by the recombination spheres around  $A$  particles. Some  $B$  particle newly created inside this prohibited volume

( $v = \gamma_d r_0^d/d$ ) recombines immediately with an  $A$  particle, which results in the reduction of the number of  $A$  particles by one, and an unchanged number of  $B$  particles (and vice versa, if  $B$  is created outside this volume). However, the limiting transition in  $1d$   $r_0 \rightarrow 0$  lifts this problem, since the accumulation kinetics turns out to be purely diffusion controlled. The relevant kinetic equations are also simplified. Using results of Ref. [21] we write the relevant kinetic equations in the following form:

$$\frac{dn(t)}{dt} = \zeta - K(t)n^2(t), \quad (22)$$

$$\begin{aligned} \partial Y(r,t)/\partial t = & \partial j(r,t)/\partial r + 2\zeta[1 - Y(r,t)]/n(t) \\ & - 2n(t)K(t)Y(r,t)[X(r,t) - 1], \end{aligned} \quad (23)$$

$$\begin{aligned} \partial X_\nu(r,t)/\partial t = & \partial j_\nu(r,t)/\partial r + 2\zeta[1 - X_\nu(r,t)]/n(t) \\ & - 2n(t)K(t)X_\nu(r,t)[Y(r,t) - 1]. \end{aligned} \quad (24)$$

Equations (22)–(24) contain a dimensionless parameter  $\zeta = \gamma_d p R^{d+2}/D$  characterizing the efficiency of particle production. This parameter could be presented in the form of a ratio  $\zeta = \tau_D/\tau_p$ , where  $\tau_D = R^2/D$  is the time for particle diffusion over the recombination sphere of radius  $R$ , and  $\tau_p \sim 1/pR^d$  is the time between two sequential events of particle creation within a sphere of the same radius  $R$ . That is, small  $\zeta$  values correspond to the situation when diffusion dominates over the particle creation, and vice versa for large  $\zeta$ . Since no particles exist before the particle source is switched on, the initial condition is  $n(0) = 0$ , i.e., the initial concentration, is no longer one of the parameters of the theory.

## VI. RESULTS

### A. Concentration decay

The kinetics of the concentration decay has been calculated for high initial concentration  $n(0) = 1$  and long dimensionless time  $t = 10^8$ . At this moment the particle concentration drops by three orders of magnitude. (Further concentration decay could hardly be measured experimentally.) To make results more obvious, in Fig. 1 we plotted not the very kinetic curves,  $n = n(t)$ , but their slopes on a logarithmic scale which defines the so-called *current critical exponents*

$$\alpha(t) = - \frac{d \ln n(t)}{d \ln t}. \quad (25)$$

To demonstrate the importance of the effect of *non-equilibrium* charge screening neglected in many previous studies, we present results for three different approximations as follows.

(i) The traditional, Debye-like treatment of the reaction kinetics with unscreened Coulomb interaction [22]. Many-particle effects are neglected, and the kinetic equations arise due to linearization of Eqs. (12)–(16) for the correlation functions. As a result, the equation for the correlation function of *similar* particles  $X_\nu(r,t)$  no longer affects the kinet-

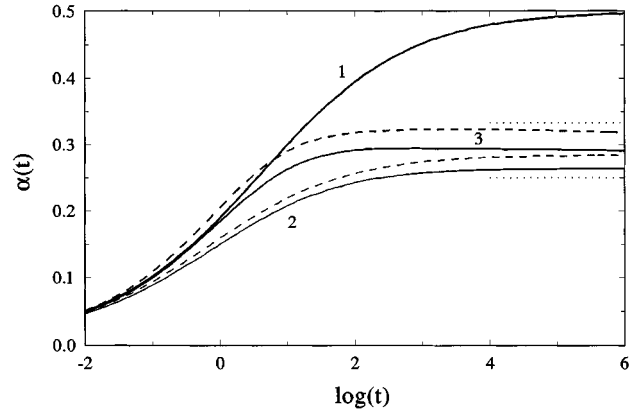


FIG. 1. The critical exponent characterizing the algebraic concentration decay, Eq. (25), as a function of dimensionless reaction time (decadic logarithm). Solid curves—symmetric reactant mobilities,  $D_A = D_B$ ; dashed curves—asymmetric mobilities,  $D_A = 0$ . Dotted lines show the two expected asymptotes:  $\alpha = \frac{1}{4}$  and  $\frac{1}{3}$ . Curves 1 correspond to the Debye theory, curves 2 to a solution of the kinetic Eqs. (12)–(16) incorporating spatial reactant correlations but neglecting dynamical charge screening, and curves 3 to the case when all screening effects are incorporated.

ics. In fact, the latter is defined entirely by the joint correlation function of dissimilar particles obeying the simple kinetic equation

$$\frac{\partial Y(r,t)}{\partial t} = \frac{\partial}{\partial r} \left\{ \frac{\partial}{\partial r} Y(r,t) + Y(r,t) \frac{\partial}{\partial r} U(r) \right\}, \quad (26)$$

where  $U(r) = -1/r$  is the unscreened Coulomb potential. After linearization of a set of kinetic equations, their solution no longer depends on the partial diffusion coefficient  $\kappa$  (solid and dashed lines in Fig. 1). At long times the solution of Eq. (26) is practically defined by the diffusion length  $\xi = \sqrt{t}$ , i.e. the decay kinetics obeys the classical algebraic law,  $n(t) \propto t^{-\alpha}$ ,  $\alpha = \frac{1}{2}$ .

(ii) The complete set of Eqs. (12)–(16) incorporating many-particle effects (via nonlinear terms) but with linearized potentials,  $U_A(r,t) = U_B(r,t) = -U(r,t) = 1/r$ . In this intermediate approximation the kinetics under study begins to depend on the mobility parameter  $\kappa$  but asymptotically it still follows the kinetics known for neutral, noninteracting particles with  $U(r) = 0$ .

(iii) The complete set of kinetic equations is combined with nonequilibrium treatment of charge screening making now no linearization. The dimensionless capillary radius was chosen as  $r_c = 0.1$ . (Its reduction to the value of 0.01 results in a small, logarithmic correction which does not affect the critical exponent.) Curve 1 in Fig. 1 shows that in the time interval considered the critical exponent rather rapidly approaches its limiting classical value of  $\frac{1}{2}$ . Curves 2, incorporating many-particle effects, approach their *quasi*-steady-state after nearly the same time, but their further approach from above to another asymptote with  $\alpha = \frac{1}{4}$  has a logarithmically slow character. For example, for the symmetrical mobilities  $\alpha(t = 10^8) = 0.264$ . In the asymmetric mobility case the deviation from the asymptote is larger,  $\alpha(t = 10^8) = 0.280$ . Such a behavior results from the long-range nature of the Coulomb interaction between particles.

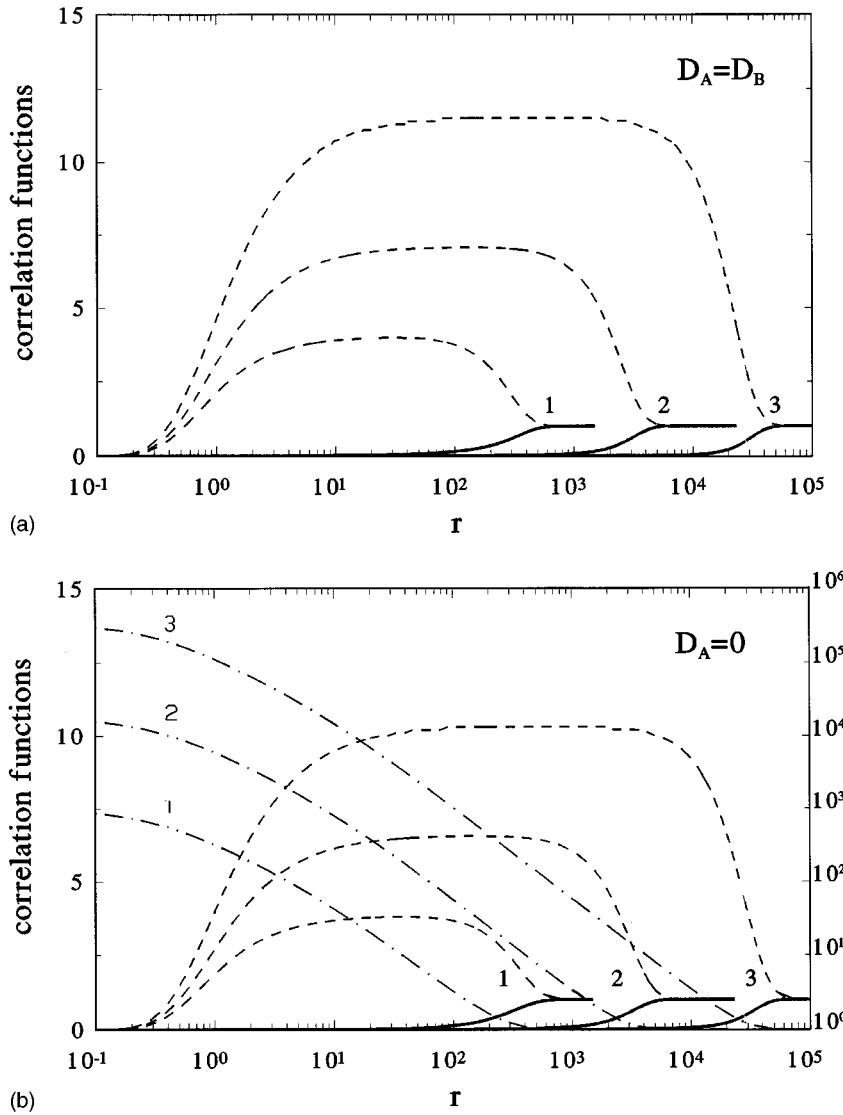


FIG. 2. The joint correlation function of dissimilar particles,  $Y(r,t)$  (solid curve), and that of similar particles,  $X_A(r,t)$  (dot-dashed curve) and  $X_B(r,t)$  (dashed curve). Curves 1–3 correspond to the dimensionless times  $10^4$ ,  $10^6$ , and  $10^8$ , respectively. (a) Symmetric mobility case,  $D_A = D_B$ . (b) Asymmetric case,  $D_A = 0$ . Note that in case (a)  $X_A(r,t) = X_B(r,t) = X(r,t)$ ; in case (b)  $X_A(r,t)$  is plotted on a logarithmic scale.

Strictly speaking, the  $\alpha = \frac{1}{4}$  law of the fluctuation-controlled kinetics in  $d=1$  is proved only for noninteracting particles [1–8]. It was generalized for interacting particles *provided* that their interaction potential is short-range and does not lead to the similar-particle collapse [10–12]. In fact, this law was proved for the case when the largest length parameter in the problem is the diffusion length, which is the case if the interaction potential is Debye-Hückel-like, as assumed in Refs. [10–12]. However, the unscreened Coulomb potential  $U(r) = -1/r$  has an *infinite* interaction radius, and thus defines the asymptotics of the correlation functions at large distances. The approach to the asymptotic character is very slow, it has a diffusion-controlled character. Moreover, in the asymmetric case there is no mechanism of smoothing the fluctuations of the immobile particle distribution at all. This is why the results of our second model of the kinetic problem are far from trivial.

Lastly, curves 3 in Fig. 1 show a considerable difference for the symmetric and asymmetric mobilities which is more pronounced than that in curves 2. However, due to a very slow approach to their limiting values, it is not clear whether and by how much the relevant critical exponents differ as  $t \rightarrow \infty$ . Arguments are given below that in the symmetric case

$\alpha = \frac{1}{4}$  (as for non-interacting particles), whereas for asymmetric mobilities the critical exponent is *larger* and the reaction occurs respectively faster,  $\alpha = \frac{1}{3}$ . Note that a similar *reaction acceleration* between charged particles with asymmetric mobilities was predicted earlier in the 3d case [14]. We found there that  $\alpha = \frac{5}{4}$ , to be compared with  $\alpha = 1$  known in the standard chemical kinetics, and  $\alpha = \frac{3}{4}$  in the fluctuation-controlled theory. Analogously, in 2d [23] we predict  $\alpha = \frac{1}{2}$  and  $\frac{3}{4}$  for symmetric and asymmetric mobilities, respectively. Before making estimates of additional critical exponents, first consider the kinetics of the pattern formation in the particle spatial distribution.

### B. Spatial reactant distributions

Figure 2 shows the time development of the joint correlation functions (note the logarithmic scale on the  $x$  axis and the same scale for immobile similar particles  $X_A$ ). A key role of the diffusion length  $\xi(t) = \sqrt{t}$  is evident here: the characteristic relative distance  $\xi'$  at which no  $AB$  pairs exist [ $Y(r < \xi', t) \ll 1$ ] increases in time as  $\sqrt{t}$ :  $\xi'$  increases by an order of magnitude as time increased by *two* orders of magnitude,  $\xi' = \xi(t)$ .

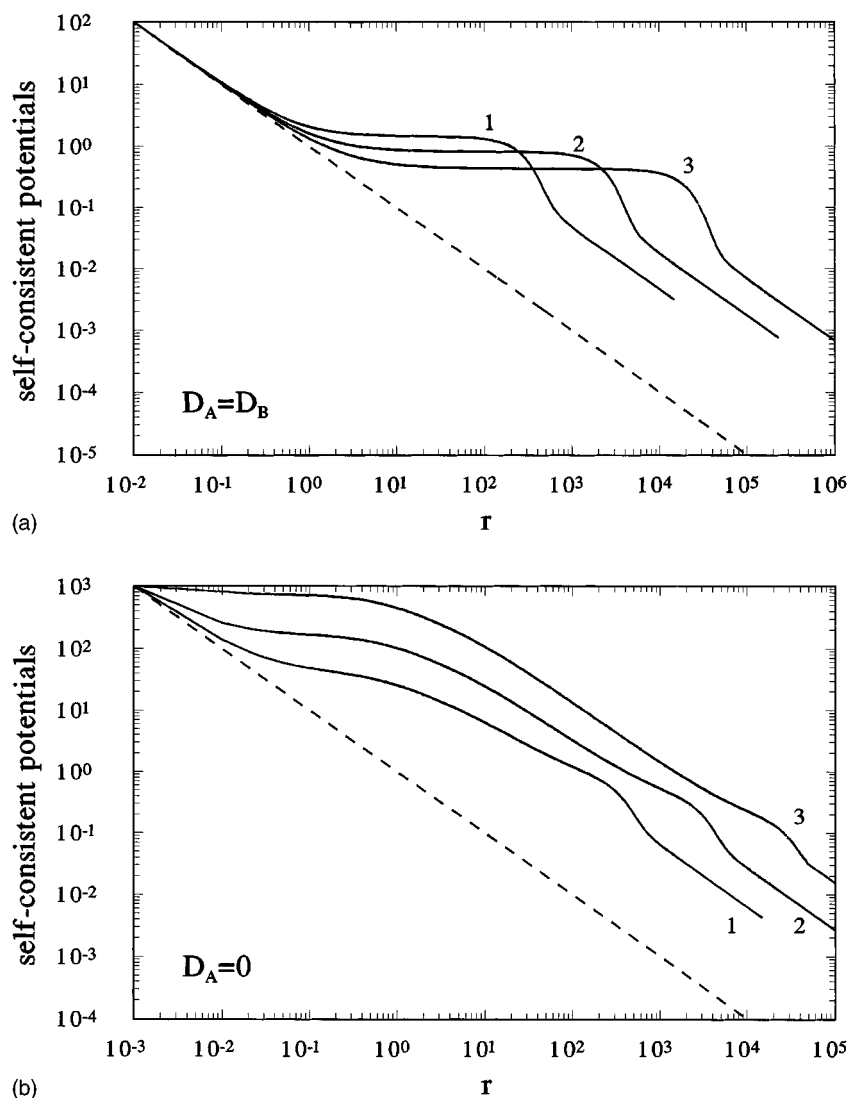


FIG. 3. Calculated self-consistent interaction energies as a function of the distance  $r$ . Solid curves 1–3 correspond to the reaction times  $10^4$ ,  $10^6$ , and  $10^8$ , respectively. The dashed curve shows the unscreened potential,  $U(r) = 1/r$ . (a) Symmetric case,  $D_A = D_B$ . Potential  $-U(r, t) = U_A(r, t) = U_B(r, t)$ . (b) Asymmetric case,  $D_A = 0$ . The potential  $-U(r, t)$  is plotted.

Irrespective of the  $\kappa$  value, the correlation functions of mobile particles  $X_\nu(r, t)$ , have a plateau at the same scale  $r < \xi'$ , and decrease rapidly to zero at  $r < 1$ . (This comes from the repulsion of similar particles at the relative distances which are short compared to the Onsager radius). In the asymmetric case the correlation functions of similar immobile particles have singularities at short  $r$ , where  $X_A(r, t)$  drops by several orders of magnitude in a narrow interval  $r \in (0, 1)$ .

A comparison of these results with earlier findings for noninteracting particles [24] shows their remarkable similarity. The main difference lies in the depletion in the correlation functions of similar mobile particles at short relative distances caused by particle repulsion, whereas for neutral particles the correlation functions are finite as  $r \rightarrow 0$ . For noninteracting particles and symmetric diffusion such a behavior of the correlation functions led to the conclusion that the *pattern formation* occurs in a form of alternating *domains* of similar particles,  $A$  or  $B$ , with linear size  $\xi(t)$  [1–7]. This reaction-induced reactant structure greatly differs from the basic assumption of standard chemical kinetics about well-stirred and homogeneous reactant distribution. In the domain, the structure reaction occurs only at the boundaries of domains of particles of different type. In the asymmetric dif-

fusion case for both noninteracting and interacting particles, mobile  $B$  reactants remain randomly distributed within their domains, whereas immobile  $A$  reactants form compact clusters—a kind of “raisins in dough” [14,24].

### C. Interaction potentials

Assuming that the kinetics of a diffusion-controlled reaction is defined by the diffusion length  $\xi(t)$ , one should expect that, in line with results presented by curves 2 in Fig. 1 the electrostatic interaction does not change the critical exponents of the reaction. However, it is demonstrated below that this is *not* true for the asymmetric diffusion case. Figure 3 shows how the effective interaction energy depends on the spatial reactant distribution. In the symmetric case (a) all energies are identical,  $U_A(r, t) = U_B(r, t) = -U(r, t)$ . For comparison the unscreened Coulomb potential,  $1/r$ , is also plotted. In the asymmetric case (b) the potential for mobile  $B$  particles remains the same as shown in case (a), and thus is not shown here. The largest change takes place for immobile  $A$  particles. However, since these particles are immobile they cannot affect the reaction kinetics, and  $U_A(r, t)$  is also omitted. The only essential potential energy remains  $U(r, t)$ .

In the symmetric case both similar ( $AA$ ,  $BB$ ) and dissimilar ( $AB$ ) particle pairs do not exist at short relative dis-

tances,  $r < 1$ , due to Coulomb repulsion and reaction, respectively. This is why the induced charge is zero and the effective potential energies coincide with the ones of the unscreened Coulomb potential. In contrast, in the interval  $1 < r < \xi(t)$  the effective potentials are constant. This means that no forces act on the particles,  $f(r,t) = -\partial U(r,t)/\partial r \approx 0$ . In other words, reactants inside domains of size  $\xi(t)$  behave as *neutral* particles since the electrostatic forces acting on any particle from other particles cancel each other. This does not take place at the domain boundaries  $r = \xi(t)$ , where dissimilar particles begin to recombine and forces  $f(r,t)$  are large. The relative motion of dissimilar particles has a form of a drift in the field created by the opposite-domain charge. This is why the potential at  $r > \xi(t)$  has very simple asymptotics,  $U(r,t) = -\xi_U/r$ , where a scale parameter  $\xi_U$  could be associated with the mean number of similar particles in the domain,  $\xi_U = N = n(t)\xi(t)^d$ . In the  $1d$  case characterized by  $\alpha = \frac{1}{4}$ ,  $\xi_U \propto \xi(t)^{1/2}$ , i.e., the length scale is in fact defined by the diffusion length but plays no significant role due to its slow growth.

#### D. Critical exponent for the asymmetric case

A qualitatively different potential behavior is observed in the asymmetric case [Fig. 2(b)]: immobile  $A$  particles do coexist at the short relative distances, and the characteristic spatial structure (raisins in dough) produces induced charge already at these short relative distances. The potential  $U(r,t)$  strongly changes its behavior—it reaches the asymptotic value of  $U(r,t) = -\xi_U/r$  already at  $r > 1$  (the Onsager radius in usual coordinates) instead of at the much larger distance, which is the diffusion length  $\xi(t)$  observed for the symmetric case [curves 3 in Fig. 3(b)]. That is, the potential  $U(r > 1, t)$  behaves like an unscreened one produced by a superparticle with a charge  $eN$  placed at the coordinate origin.

It is convenient to use dimensional scale parameters. As was mentioned above, in  $3d$  the effective radius for interacting particles,  $R_{\text{eff}}$ , is the larger of the two: the contact radius  $r_0$  or the Onsager radius  $R$  [22]. Usually  $R \gg r_0$ , and the latter determines the reaction kinetics. In our  $1d$  case we set  $r_0 = 0$ , and  $R$  remains the *only* length scale of the problem (from the point of view of standard chemical kinetics). Incorporation of many-particle effects brings another scale parameter into the kinetics under study—the diffusion length  $\xi(t)$ . As follows from curves 2 in Fig. 1, the long-time kinetics is defined by the largest scale, which is now  $\xi(t)$ .

The  $1d$  reaction asymptotics with  $\alpha = \frac{1}{4}$  means not only the relevant concentration decay law,  $n(t) \propto t^{-1/4}$ , but also the asymptotics of the reaction rate,  $K(t) \propto t^{-3/4}$ , Eq. (2). The reaction rate  $K(t)$  is the structural characteristic of the system, since it is determined by the gradient of the correlation function  $Y(r,t)$  and thus should be asymptotically a simple function of the characteristic lengths of the problem,  $R$  and  $\xi(t)$ . Their only combination of length dimension is  $K(t) \propto DR^{1/2}/\xi(t)^{3/2}$ .

In the asymmetric case a superparticle consisting of immobile  $A$  particles should be characterized by another reaction radius,  $R_{\text{eff}} = NR$  instead of  $R$  (recall that the Onsager radius is proportional to the product of particle charges). Combining the above-derived expression for the reaction rate

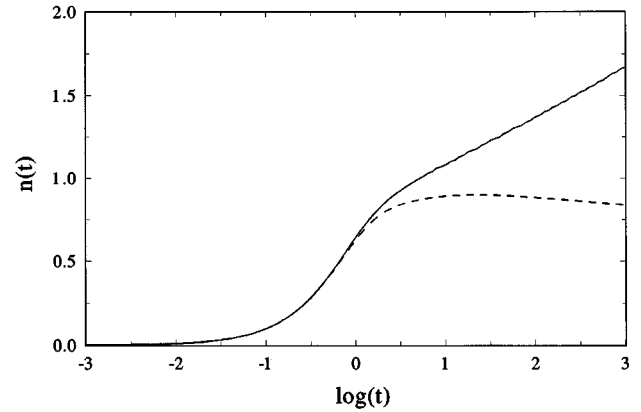


FIG. 4. The accumulation kinetics for the symmetric case,  $D_A = D_B$  (solid curve), and the asymmetric case,  $D_A = 0$  (dashed curve) (decadic logarithm).

with  $R_{\text{eff}}$ , one obtains that  $K(t) \propto DR_{\text{eff}}^{1/2}/\xi(t)^{3/2}$ . Keeping in mind that  $N = n(t)\xi(t)$ , its substitution into Eq. (2) in the  $1d$  case gives us the critical exponent  $\alpha = \frac{1}{3}$ . In other words, in the asymmetric case the reaction kinetics is accelerated as compared to *both* the noninteracting particles and the symmetric case of interacting particles ( $\alpha = \frac{1}{4}$ ). This confirms our previous results for the  $3d$  case [14].

#### E. $2d$ case

Let us compare now very briefly the main differences between the  $1d$  and  $2d$  cases (the latter to be discussed in detail elsewhere [23]). The  $2d$  kinetics was studied until  $t = 10^6$ , when the concentration decreases by four orders of magnitude.

(i) The Debye theory predicts the classical critical exponent,  $\alpha = 1$ . Our treatment of the unscreened Coulomb interaction (analog of curves 2 in Fig. 1) yields  $\alpha = \frac{1}{2}$ , the same as obtained earlier for noninteracting particles. Incorporation of nonequilibrium screening (many-particle effects) into the effective interaction potentials results in the splitting of the kinetic curves,  $\alpha = \alpha(t)$ , for the symmetric and asymmetric cases. In the former case the reaction asymptotics remains the same as for neutral particles, whereas in the latter case we expect a larger value of  $\alpha = 3/4$ . In all cases the approach to the asymptotic values is very slow.

(ii) The behavior of the correlation functions is essentially the same as in  $1d$ .

(iii) The effective potentials remind us of those shown in Fig. 3, but with different asymptotics. In the symmetric case the scale parameter  $\xi_U$  coincides with the diffusion length, whereas in the asymmetric case  $\xi_U/\xi(t) \rightarrow 0$ , since the concentration decays faster than in the symmetric case.

#### F. Accumulation kinetics

The accumulation kinetics was calculated for the following parameters:  $\zeta = 1$ ,  $r_c = 0.1$ , and  $n(0) = 0$ . Figure 4 demonstrates that our microscopic kinetics differs considerably from the results of mesoscopic theory [10–12] predicting algebraic concentration growth,  $n(t) \propto t^\alpha$  with  $\alpha = \frac{1}{5}$ . In contrast, our study shows that in the symmetric case  $n(t)$  increases only logarithmically over three orders of magnitude

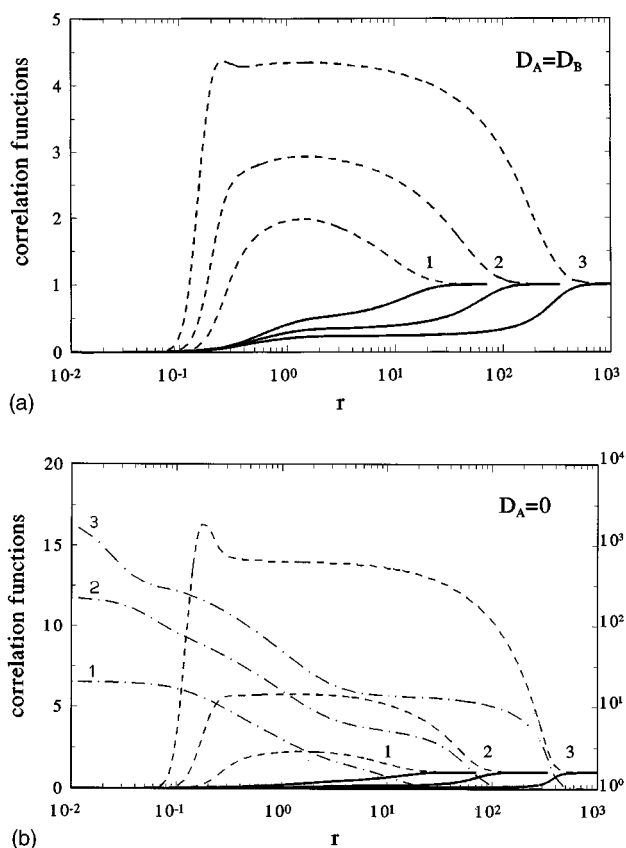


FIG. 5. The joint correlation function of dissimilar particles,  $Y(r,t)$  (solid curve), and that of similar particles,  $X_A(r,t)$  (dot-dashed curve) and  $X_B(r,t)$  (dashed curve). Curves 1–3 correspond to the dimensionless times  $10^1$ ,  $10^2$ , and  $10^3$ , respectively. (a) Symmetric case,  $D_A = D_B$ . (b) Asymmetric case,  $D_A = 0$ . Note that for case (a)  $X_A(r,t) = X_B(r,t) = X(r,t)$ , whereas for case (b),  $X_A(r,t)$  is plotted on a logarithmic scale.

in time. In the asymmetric case  $n(t)$  reaches a *maximum* and then decreases slowly. The former case reminds us of the  $2d$  case for neutral particles (logarithmic growth) [21], whereas the latter case is qualitatively similar to the  $3d$  case (the same concentration saturation). This behavior could be understood qualitatively assuming that similar-particle repulsion is analogous to the finite size of particles due to which similar particles cannot approach each other to within a distance less than some critical value.

This is supported by the behaviour of the correlation functions (Fig. 5). Similarly to the concentration decay (Fig. 2) the domain structure is characterized by the diffusion length  $\xi$ . At  $t > 1$  the reactant concentration is high,  $n(t) \sim 1$  and the domain volume is densely filled by particles. This results in large induced charge. Mobile  $B$  particles repel each other and do not exist at the relative distances  $r < 0.1$ . If recently created  $B$  particles are produced closely to preexisting  $B$  particles, they also repel each other. This results in the appearance of a local maximum in the correlation functions,  $X_B$ , at  $r < 0.1$ , well seen at  $t = 10^3$ . For immobile  $A$  particles such an effect does not take place—these particles form dense clusters—Fig. 5(b). At high concentrations mobile  $B$  particles due to their repulsion drift to the domain boundaries at which reaction takes place. This is why a slow concentration growth occurs mainly due to  $AB$  particle *segregation*:

domain sizes increase as  $\xi$ , and their surface decreases (where the reaction takes place). Coulomb repulsion of similar particles preventing the formation of their dense aggregates is not completely equivalent to a hard-sphere model of finite-size particles. In fact, if the domain size is fixed, a permanent production of similar particles inside the domain volume would lead to an infinite growth of the concentration and thus to a decrease of the minimum distance between particles. This is why the restriction of dense-aggregate formation is related to the domain *surface*.

A simple estimate of the number of particles inside a domain,  $N = n(t)\xi(t)^d$ , even assuming for the reactant concentration  $n(t) = \text{const}$ , gives an important result which follows from the potential asymptotics  $U(r) = -\xi_U/r$ . The scale parameter  $\xi_U$  in the  $1d$  case coincides with the diffusion length  $\xi(t)$ , i.e. at large  $r$  the effective potential reveals a scaling behavior  $U(r,t) \propto (r/\xi(t))^{-1}$ . In this case one naturally should expect a change of the asymptotic reaction law as compared to the case of both noninteracting particles and particles with a short-range potential.

Note that under the algebraic concentration growth predicted by mesoscopic theory the parameter  $\xi_U$  at some time would exceed the diffusion length and thus become a *control parameter* determining the accumulation kinetics. This is why the condition  $\xi_U = \xi(t)$  is a *crossover* between diffusion- and non-diffusion-controlled reactions. From this condition comes the observed restriction of the concentration growth (see Fig. 4).

## VII. DISCUSSION AND CONCLUSION

We compare in the conclusion the main results of the mesoscopic [10–12] and the present, microscopic formalism for the diffusion-controlled  $A + B \rightarrow 0$  reaction between charged particles in the  $1d$  case. The former theory claims that the critical exponents in the concentration algebraic decay is the same for charged and neutral particles, *provided*, (i) similar particles ( $AA$ ,  $BB$ ) repel each other, and (ii) the pair interaction potential is not divergent (e.g. like the Debye-Hückel potential).

The microscopic theory generalizes this result (valid for the case of symmetric particle mobilities) for the *unscreened* (divergent) Coulomb potential. Moreover, we have studied the case of asymmetric mobilities ( $D_A = 0$ ,  $D_B > 0$ ) and predicted reaction acceleration, i.e., the existence of a critical exponent  $\alpha = \frac{1}{3}$ . We demonstrated that this peculiarity is a direct consequence of the specific spatial distribution of reactants studied by us in terms of the joint correlation functions for both similar and dissimilar reactants.

A large discrepancy between the two approaches is found for the accumulation kinetics under a permanent particle source. Unlike the mesoscopic prediction of the infinite concentration growth  $n(t) \propto t^\alpha$ , for point particles with the equilibrium Debye-Hückel potential, we observe a much slower, logarithmic growth—in the case of symmetric mobilities, and concentration quasisaturation for asymmetric mobilities. This is a direct consequence of the fact that the use of a model, equilibrium Debye-Hückel potential is not justified. In fact, the effective potential should be related to the spatial distribution of reactants which makes it time dependent and nonequilibrium.

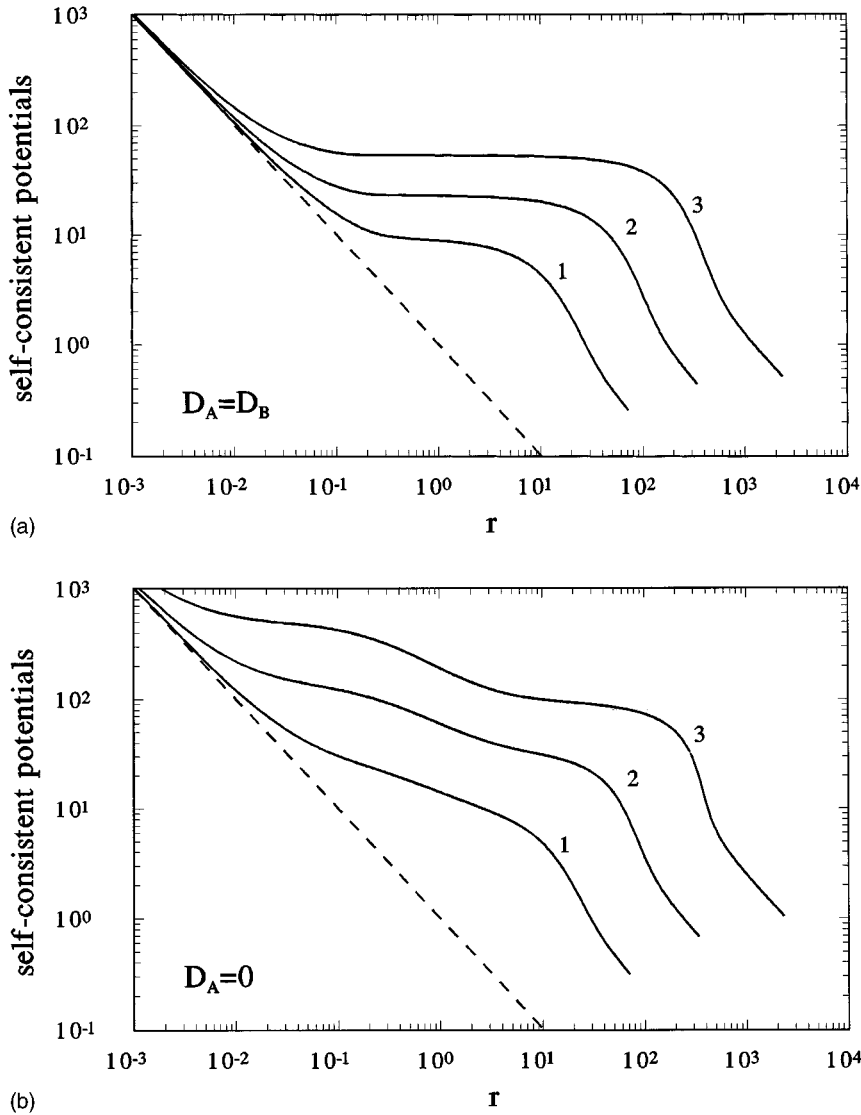


FIG. 6. Self-consistent potentials in the accumulation kinetics. Solid curves 1–3 correspond to the reaction times  $10^1$ ,  $10^2$ , and  $10^3$ , respectively. The dashed curve is the Coulomb potential  $U(r) = 1/r$ . (a) Symmetric case,  $D_A = D_B$ . Potential  $-U(r, t) = U_A(r, t) = U_B(r, t)$ . (b) Asymmetric case,  $D_A = 0$ . The potential  $-U(r, t)$  is plotted.

Our study [23] of the  $2d$  case shows a very different situation: at long times both the particle concentration and the correlation functions reveal *steady-state* behaviour, practically independent on the diffusion length  $\xi(t)$ . This could be understood following our previous qualitative analysis: in  $2d$  the crossover condition  $\xi_U = \xi(t)$  cannot be realized (assuming that the behaviour of the correlation functions is defined by the diffusion length).

#### ACKNOWLEDGMENTS

This research was supported by the Deutsche Forschungsgemeinschaft (via financial support for V. N. Kuzovkov), by the European Community Human Capital and Mobility network on the Solid State Atomic Scale Simulations, and in part by the Fonds der Chemischen Industrie. The authors are indebted to A. Blumen, H. Fogedby, and I. Sokolov for stimulating discussions.

#### APPENDIX

Numerical calculation of the effective potentials, Eq. (21), could be done using the trapezoid method. There are no problems here except for a long computational time as com-

pared to the  $3d$  case [14], where numerical solution of the relevant differential Eq. (9) could be easily done. Numerical solution of ordinary differential equations (12) and (22) is also trivial. The main problem arises due to the necessity of solving nonlinear, partial differential Eqs. (13), (15) or (23), (24) with singular potentials.

To illustrate our method of their solution, consider the typical equations

$$\partial g(r, t) / \partial t = \partial j(r, t) / \partial r - h[g, r, t]g(r, t), \quad (\text{A1})$$

$$j(r, t) = \partial g(r, t) / \partial r + \partial U[g, r, t] / \partial r g(r, t). \quad (\text{A2})$$

Here  $h[g, r, t]$ ,  $U[g, r, t]$  are functionals of  $g(r, t)$  sought for, and  $U[g, r, t]$  has a singularity in  $r$ :  $U[g, r, t] = 1/r$  as  $r \rightarrow 0$ . After the discretization of the equation using a standard method,  $r_i = i\Delta r$ ,  $t_m = m\Delta t$ ,  $g(r_i, t_m) = g_i^0$ ,  $g(r_i, t_{m+1}) = g_i$ , and  $h(g, r_i, t_{m+1}) = h_i(\bar{g})$ , we arrive at the difference equation which could be presented in a quasilinearized traditional form

$$a_i[\bar{g}]g_{i-1} + b_i[\bar{g}]g_{i+1} - c_i[\bar{g}]g_i - h_i(\bar{g})g_i - g_i/\Delta t = -g_i^0/\Delta t, \quad (\text{A3})$$

where coefficients  $a_i$ ,  $b_i$ , and  $c_i$  arise due to the approximation of  $\partial j(r,t)/\partial r$ . These coefficients depend on  $U[g,r,t]$ , and thus are functionals of  $g$ . Solution of Eq.(A1) is obtained by means of quasi-linearization:  $\bar{g}_i = g_i^0$  is used as initial guess, Eq.(A1) is solved in the standard way, then we substitute  $\bar{g}_i = g_i$ , and the iterative process continues until convergence is achieved within a required tolerance. In this way we avoid a problem of the nonlinearity of the kinetic equations.

The approximation of  $\partial j(r,t)/\partial r$  is less trivial. Use of finite differences for derivatives fails for the singular potentials since negative coefficients  $a_i$  or  $b_i$  become so large that this cannot be compensated for by any reduction of the time increment,  $\Delta t$ . We suggested the procedure where always  $a_i, b_i, c_i \geq 0$ . This allows to perform calculations for sufficiently large  $\Delta t$  values. This is of key importance for determining the asymptotic ( $t \rightarrow \infty$ ) kinetic law.

The procedure is as follows. To obtain a conservative difference scheme, the integral in the interval  $r \in [r_{i-1/2}, r_{i+1/2}]$  with  $r_{i\pm 1/2} = (i \pm 1/2)\Delta r$  reads

$$\int (\partial j/\partial r) dr = j_{i+1/2} - j_{i-1/2}. \quad (\text{A4})$$

In the equation for the flux density  $j = \partial g/\partial r + (\partial U/\partial r)g$  substitution  $g = \exp(-U)\omega$  gives  $j = (\partial\omega/\partial r)\exp(-U)$ . It is

important that the exponent  $\exp(U)$  has the argument  $U$  rapidly changing on the scale  $\Delta r$  and thus also changes rapidly as compared to the slowly varying functions  $j$  and  $\partial U/\partial r$ . This is why the integral

$$\int j \exp(U) dr = \omega_i - \omega_{i-1} \quad (\text{A5})$$

could be estimated in the interval  $r \in [r_{i-1}, r_i]$  as

$$\begin{aligned} \int j \exp(U) dr &\approx j_{i-1/2}/(\partial U/\partial r)_{i-1/2} \int \exp(U) dU \\ &= j_{i-1/2}/(\partial U/\partial r)_{i-1/2} (\exp(U_i) - \exp(U_{i-1})) \\ &\approx j_{i-1/2} \frac{(\exp(U_i) - \exp(U_{i-1}))}{(U_i - U_{i-1})} \Delta r. \end{aligned} \quad (\text{A6})$$

Now returning from the intermediate function  $\omega$  to  $g$  sought for, one obtains the basic relation for the difference scheme coefficients

$$j_{i-1/2} = (g_i \exp(\Psi_i) - g_{i-1}) \frac{\Psi_i/\Delta r}{\exp(\Psi_i) - 1}, \quad (\text{A7})$$

where  $\Psi_i = U_i - U_{i-1}$ . As it should be, the flux density depends not on the very potential  $U$  but on its derivative  $\Psi_i = \Delta r (\partial U/\partial r)$  at  $r = r_{i-1/2}$ . The expression derived is also used in determining the reaction rate  $K(t)$ , Eq. (12), and for the boundary conditions imposed on Eq. (17).

- 
- [1] D. Toussaint and F. Wiczek, *J. Chem. Phys.* **78**, 2642 (1983).  
 [2] A. A. Ovchinnikov and Ya. B. Zeldovich, *Chem. Phys.* **28**, 215 (1978).  
 [3] K. Lindenberg, B. J. West, and R. Kopelman, *Phys. Rev. Lett.* **60**, 1777 (1988).  
 [4] K. Kang and S. Redner, *Phys. Rev. Lett.* **52**, 955 (1984); *Phys. Rev. A* **32**, 435 (1985).  
 [5] V. N. Kuzovkov and E. A. Kotomin, *Chem. Phys.* **76**, 479 (1983); **81**, 335 (1983); **98**, 351 (1985).  
 [6] V. N. Kuzovkov and E. A. Kotomin, *Rep. Prog. Phys.* **51**, 1479 (1988).  
 [7] E. A. Kotomin and V. N. Kuzovkov, *Rep. Prog. Phys.* **55**, 2079 (1992).  
 [8] Special issue of *J. Stat. Phys.* **65** (5/6) (1991).  
 [9] H. Eyring, S. H. Lin, and S. M. Lin, *Basic Chemical Kinetics* (Wiley, New York, 1980).  
 [10] I. M. Sokolov and A. Blumen, *Europhys. Lett.* **21**, 885 (1993).  
 [11] I. M. Sokolov, P. Argyrakis, and A. Blumen, *Fractals* **1**, 470 (1993).  
 [12] I. M. Sokolov, P. Argyrakis, and A. Blumen, *J. Phys. Chem.* **98**, 7256 (1994).  
 [13] V. N. Kuzovkov and E. A. Kotomin, *Physica A* **192**, 172 (1992).  
 [14] V. N. Kuzovkov and E. A. Kotomin, *J. Stat. Phys.* **72**, 145 (1993).  
 [15] V. N. Kuzovkov and E. A. Kotomin, *J. Chem. Phys.* **98**, 9107 (1993).  
 [16] M. N. Kabler, in *Point Defects in Solids*, edited by J. Crawford (Plenum, New York, 1972), Vol. 1, Chap. 4.  
 [17] V. N. Kuzovkov and E. A. Kotomin, *J. Phys. Condens. Matter* **7**, L481 (1995).  
 [18] E. A. Kotomin, V. N. Kuzovkov, M. Zaiser, and W. Soppe, *Radiat. Eff. Defects Solids*, **136**, 209 (1995).  
 [19] J. G. Kirkwood, *J. Chem. Phys.* **76**, 479 (1935).  
 [20] R. Balescu, *Equilibrium and Non-equilibrium Statistical Mechanics* (Wiley, New York, 1975).  
 [21] V. N. Kuzovkov and E. A. Kotomin, *Phys. Scr.* **47**, 585 (1993).  
 [22] P. Debye, *J. Electrochem. Soc.* **32**, 265 (1942).  
 [23] V. N. Kuzovkov, E. A. Kotomin, and W. von Niessen, *J. Chem. Phys.* (to be published).  
 [24] E. A. Kotomin, V. N. Kuzovkov, W. Frank, and A. Seeger, *J. Phys. A* **27**, 1453 (1994).